A rational method for assessing the occurrence of brittle failure in deep tunnels

International Society for Rock Mechanics and Rock Engineering
Norwegian Group for Rock Mechanics

ISRM International Symposium
Eurock 2025 – Expanding the Underground Space
Trondheim, Norway, 16-20 June
ISBN 978-82-8208-079-8

A rational method for assessing the occurrence of brittle failure in deep tunnels

A. Insana, L. Milan, M. Barbero, M. Barla, M. Borri-Brunetto, & D. Martinelli
Politecnico di Torino, Torino, Italy
lorenzo.milan@polito.it (email of corresponding author)

Abstract

If not properly predicted and accounted for during the tunnel design process, brittle failure can lead to time, cost and safety issues. To support designers in addressing these dangerous and critical phenomena, this paper presents a suggested design process for deep tunnels with suspected brittle failure potential. The strength of this approach is that it enables understanding whether brittle failure is likely during excavation and, if so, predicting its magnitude.

The first step is to apply the recently developed and presented Tunnel Brittleness Index (TBI). TBI quantifies the potential of ductile and brittle failure around deep tunnels by analyzing the competition between the two failure mechanisms. The collection of the input parameters needed to calculate TBI will be described, and its operating principles will be recapped.

When brittle failure mechanism results predominant over the ductile one, based on the TBI calculation, numerical analyses by the hybrid Finite-Discrete Element Method (FDEM) represent a powerful tool to address its occurrence and intensity at the site. Hence, the execution of such analyses to study the site-scale problem constitutes the second step of the suggested design process. The main aspects to be careful to when performing such analyses will be outlined.

After describing the steps of the methodological approach, the case study of the Turin-Lyon Base tunnel will be addressed to demonstrate its applicability.

Keywords

Brittle failure, deep tunnels, brittleness index, numerical modelling, FDEM

1 Introduction

In recent years, the construction of underground caverns and tunnels at significant depths has become increasingly common, reflecting the growing demand for the utilization of subterranean spaces (Cai 2013; Gong et al. 2020; Askaripour et al. 2022). A key challenge associated with deep tunnels is the intense natural stress present at such depths. This results in substantial deviatoric stress during the excavation process, which could induce the rock mass failure.

When the rock mass can be modelled as an equivalent continuum medium, failure modes around deep tunnels can generally be categorized into two main types, ductile or brittle. This distinction depends on the rock's strength and deformability properties, as well as the applied stresses. Ductile failure involves a gradual plastic deformation of the rock mass surrounding the tunnel, leading to increasing inward radial displacement. In some situations, gravity-driven collapses of small volumes of fractured material from the crown or sidewalls into the cavity may occur. Since the strength of the rock mass does not diminish drastically once it surpasses the elastic limit, this type of failure tends to progress relatively slowly. Conversely, brittle failure is associated with sudden, violent phenomena. It is encountered when excavating a tunnel in hard, high-strength rock masses (massive to moderately jointed), subjected to high in situ stresses, at high depth. Such failure takes place due to the creation, growth, and accumulation of micro- and macro-cracks in the parietal areas parallel to the excavation boundary, induced by the redistribution of stresses following the excavation. Such a stress-driven process is called spalling (Martin et al. 2003). A characteristic of stress-induced failure of tunnels in brittle rock is the notched-V shape of the failure region linked to tunnel face advance. The associated slabbing and spalling initiate where tangential compressive stress is highest, in correspondence with the minor principal stress axis.

Rapid fracturing and destabilization of the rock are accompanied by significant energy releases, which may vary in intensity (Diederichs 2007; Cai 2013; Cai and Brown 2017; Gong et al. 2020). Less violent forms of brittle failure, such as slabbing and spalling, result in the detachment and fall of smaller, low-velocity rock blocks. Slabs can range in thickness from a few millimetres to tens of centimetres and, with large openings, can be several square metres in surface area (Martin et al. 1997; Ortlepp 1997). The extent and depth of failure are a function not only of the fracture network but also of the ratio between the in-situ stress magnitude and the rock mass strength. In contrast, the most severe form of brittle failure—rockburst—poses a serious risk. Rockbursts are events involving the failure and ejection of rock fragments at high velocities into the tunnel, due to a dramatic release of energy (Cook 1976; Kaiser et al. 1996; Ortlepp 1997; Hoek et al. 2000; Li et al. 2017). During excavation, the surrounding rock experiences a rapid release of pressure, causing the stored strain energy to trigger fracturing and explosive failure as the rock seeks to establish a new equilibrium state (Liu et al. 2018; Liang et al. 2013). The ejection of rock blocks during a rockburst can result in project delays, financial losses, structural collapses, equipment damage, and, in severe cases, injuries or fatalities (Naji et al. 2019; Chen et al. 2021). The velocity of these ejected blocks typically reaches up to 7–10 m/s according to Ortlepp (2001), but smaller fragments can travel at speeds of up to 50 m/s (He et al. 2022). Rockbursts are driven by the accumulation of high deviatoric stresses around excavations, which intensify with increasing depth. Additionally, they are most commonly observed in massive, hard rock formations capable of storing significant amounts of strain energy (Ortlepp 1994; Li et al. 2012; He et al. 2015). Depending on the in-situ state of stress and the confinement level at the excavation boundary, spalling and/or rock-bursting, can alternatively develop. Knowing the extent of these processes is crucial for rock support design.

Therefore, it is important to properly predict and account for brittle failure during the tunnel design process, to prevent time, cost and safety issues. With the aim of supporting designers in addressing these dangerous and critical phenomena, this paper presents a design procedure for deep tunnels susceptible to brittle failure. The strength of this approach is that it enables understanding whether brittle failure is likely during excavation and, if so, predicting its magnitude. In the following, the main steps of the suggested design method are outlined and are then applied to the case study of the Turin-Lyon Base tunnel.

2 A methodology for assessing brittle failure in deep tunnels

A methodological overview of the suggested procedure for the study of brittle failure in deep tunnels is given in Fig. 1. The flow is divided into two main blocks. The first block is devoted to the qualitative

prediction of the proneness to brittle failure of the rock mass around deep tunnels. It involves the calculation of a recently introduced index named Tunnel Brittleness Index (Milan 2024a; Milan et al., 2025) whose main peculiarities will be described in Section 3. The second block is activated when the outcome of the first block is that brittle failure is predominant. It deals with the quantification of brittle failure magnitude and extension by means of numerical modelling that will be described in Section 4.

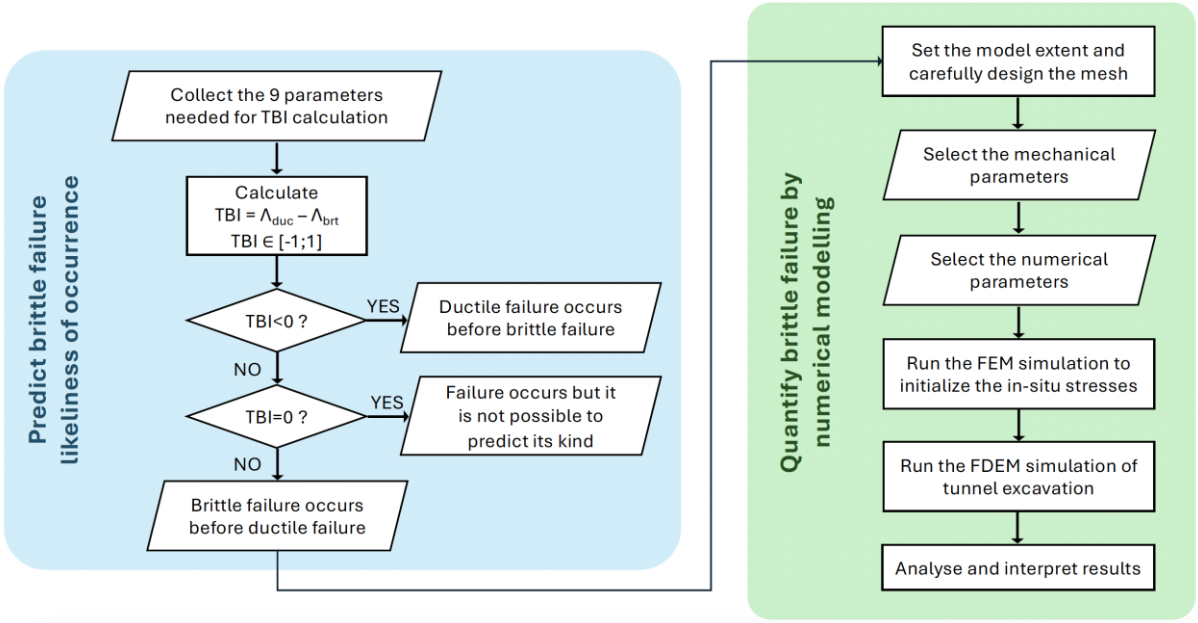

Fig. 1 Flow chart of the suggested methodology to predict and quantify brittle failure in deep tunnels.

3 Evaluation of the Tunnel Brittleness Index

The Tunnel Brittleness Index (TBI) is a novel tool for predicting ductile or brittle failure around deep tunnels in the early stages of the design, which can be crucial in the preliminary choice of excavation techniques and machinery, as well as the support systems. The index is based on the concept of competition between two opposing damage mechanisms: ductile and brittle failure. This methodology employs the analytical solutions of two distinct mechanical models specifically developed to describe the rock damage associated with these failure mechanisms. Ductile and brittle failure are considered to be driven by the stress release resulting from the excavation of a deep tunnel.

The two models focus on the cross-section of a circular tunnel, simulating the excavation process using the confinement-convergence method. As well known, the 3D excavation process is simulated by applying a continuously decreasing fictitious internal pressure to the tunnel contour. When the internal pressure is such that failure occurs in the surrounding rock mass, its value is referred to as the critical pressure. Two distinct critical pressures can be calculated depending on whether the rock mass exhibits brittle or ductile failure. These calculations form the basis of TBI, which quantifies the rock's tendency toward brittle failure by analysing the stress and energy changes induced by the excavation and subsequent failure mechanisms. The index thus measures the predominance of one failure mode over the other.

The competition between ductile and brittle failure is assessed by identifying the type of failure that occurs first during the stress reduction process. The reduction of the fictitious internal pressure is governed by an unloading parameter, Λ, that ranges from 0 (representing the initial, unexcavated state) to 1 (indicating excavation completion). During this process, failure can occur at specific points around the tunnel, and the unloading parameter value at the onset of failure is termed critical. TBI is defined as the difference between the critical unloading parameters for brittle failure (Λ_{brt}, calculated using a fracture mechanics approach) and ductile failure (Λ_{duc}, evaluated through an elastic-plastic model). The detailed description of the two mechanical models and the calculation of the two critical Λ values can be found in Milan (2024a).

TBI ranges from -1 to 1, with its absolute value indicating the dominance of one failure mode over the other. Depending on the calculated value, the results can be classified into the following scenarios:

- The value TBI=0 corresponds to the condition $\Lambda_{brt} = \Lambda_{duc}$, which means that the tunnel failure occurs for the same Λ value regardless of the failure mode. Failure occurs but it is not possible to predict its type
- TBI>0 implies that $\Lambda_{brt} < \Lambda_{duc}$, that is, during the excavation process, brittle failure occurs before ductile failure
- TBI<0 implies that $\Lambda_{brt} > \Lambda_{duc}$, in this case ductile failure occurs before brittle failure.

TBI depends on nine input parameters, as outlined in Table 1. To facilitate rapid computation, a standalone executable application was developed (Milan, 2024b). During the computation process, specific critical scenarios are addressed, particularly those related to certain values of Λ_{duc} and Λ_{brt}. In some cases, the calculations may yield inadmissible values for one or both Λ parameters - such as values exceeding 1, negative values, or even imaginary numbers - which lack physical significance. These outcomes indicate that the input parameter combination does not support the occurrence of the analysed failure mechanisms. Specifically:

- If Λ_{duc} is inadmissible and Λ_{brt} is valid, the value TBI=1 is forced, indicating the maximum prevalence of the brittle failure mechanism over the ductile one. This condition corresponds to the maximum brittleness of the rock-tunnel system.
- If Λ_{brt} is inadmissible and Λ_{duc} is valid, the value TBI=-1 is forced, indicating the maximum prevalence of the ductile failure mechanism over the brittle one. This condition corresponds to the maximum ductility of the rock-tunnel system.
- The case in which both Λ_{duc} and Λ_{brt} are inadmissible is handled by forcing TBI=NaN (Not a Number). This is a situation in which failure is not predicted by either of the two damage models used, so the TBI index is not applicable.

Table 1 Input parameters to calculate TBI.

Parameter group	Parameter	Description
1 – Rock parameters	E	Young's modulus of the rock mass
	ν	Poisson's ratio of the rock mass
	λ	Equivalent thickness of the rock
	A	Strength parameter of the Drucker-Prager failure criterion of the rock mass
	B	Strength parameter of the Drucker-Prager failure criterion of the rock mass
	G_i	Intact rock shear modulus
	G_f	Intact rock fracture energy
2- Stress state	σ_∞	Maximum principal geostatic stress
	k	In situ stress ratio

4 Numerical modelling of brittle failure in tunnels by FDEM

The combined Finite Discrete Element Method (FDEM) was originally created with the specific objective of bridging the gap between continuum and discontinuum methods (Munjiza et al. 1995). Finite element-based analysis was combined with discrete element-based transient dynamics analysis, contact detections-interaction algorithms and a fracture model accounting for the onset and propagation of new cracks as well as the progressive extension of pre-existing discontinuities. The possibility to track the onset and the development of fractures and, at the same time, to properly identify its progression towards failure represents an important added value for rock engineering design.

However, some aspects need special care and are peculiar for modelling with FDEM: the definition of specific numerical parameters and mesh discretisation. Input data differ from what is needed in a continuum or a purely discontinuum analysis. In addition to the usual elemental properties affecting the bulk material response (Elastic modulus E, Poisson's ratio ν, density ρ) and strength properties (internal cohesion c, internal friction angle Φ, tensile strength σ_t), the values of specific numerical and mechanical parameters (viscous damping; normal, tangential and fracture penalty; Mode I and Mode II fracture energy) need to be selected carefully. These parameters can largely influence the results of the simulations. Moreover, the mesh needs to be carefully discretised so that its influence on the results (in terms of fracturing patterns) is minimised.

The simulation of damage and fractures is achieved by means of specific four-node cohesive crack elements which are inserted along the edges of the triangular finite elements (Mahabadi et al. 2012;

Lisjak et al. 2013; Tatone and Grasselli 2015). Therefore, the onset and the propagation of fractures are constrained by the mesh topology, since only inter-element fracture is allowed, and no adaptive remeshing algorithms are implemented. Localization of fractures therefore depends directly on the discretization of the domain and on the element size. To limit the mesh induced bias on the fracture processes, it is therefore necessary to use small elements size compared to the modelled domain. In particular, the mesh should be finer in regions of high stress/strain gradients and expected fracturing, and characterized by a smooth element size transition when grading it from fine to coarse. At the same time, a random, unstructured mesh discretization should be adopted in place of structured ones. The adoption of sufficient small element size is hence required to overcome the mesh sensitivity of the FDEM. However, a decrease of the elements size entails a reduction of the time step size of the simulation and an increase of the total number of time steps, therefore of the computational time (Piovano et al. 2011; Barla et al. 2012).

After selecting appropriate mesh, mechanical and numerical parameters, in-situ stress initialization and boundary conditions assignment can take place. In deep tunnels, gravity gradient can be neglected, as it would be done with other numerical methods. The in-situ stress field can be simply obtained by specifying the three independent values of the Cauchy's stress tensor in the *x*, *y* reference system. The total number of time steps for this initialization needs to be specified as well (explicit integration of the equation of motion). Absorbing boundary conditions can be enabled to dissipate dynamic oscillations and accelerate convergence during the geostatic initialization.

First, a Finite Element analysis is run where crack elements are not generated. After stepping to elastic equilibrium, the initial state of stress is applied and the nodal coordinates calculated by the FEM solver are used as input for the following FDEM run. The updated nodal coordinates and velocities obtained at the end of each phase need to be used as the input for the subsequent simulation step.

Then, fracture is activated and the tunnel excavation is simulated. Previous published works highlighted the need to closely control the excavation process to correctly reproduce the induced stress release (Lisjak et al. 2014) to avoid dynamic artefacts and unrealistic fractures. A core replacement technique can be adopted to capture the three-dimensional tunnel face advancement effect and progressive deconfinement of the rock mass.

After the above stages, the fracture evolution and the final pattern retrieved after the excavation of the deep unsupported tunnel can be observed to evaluate the extension (spalling depth) and shape of the fractured area around the cavity. Enough time steps are needed to capture the crack propagation.

When support measures need to be included in the model (e.g. shotcrete lining), it is possible to represent the lining by a layer of constant-strain triangular elements with specific properties. Available commercial FDEM software also implemented structural elements such as rockbolts.

5 Application to a case study

The methodological design process outlined in Fig. 1 is here applied to the case study of the Turin-Lyon tunnel, which will be part of a new railway line to connect the two cities. The main infrastructure of the Turin-Lyon 270 km-long connection is the Mont Cenis Base tunnel, a 57.5 km long, twin-tube, single-track tunnel which will allow crossing the Alps with overburdens of more than 2000 m. The tunnel's diameter is 10.4 m. The tunnel will pass through an extremely complex geological context in terms of lithological variety and geomechanical-hydrogeological features and will reach its maximum depth below the Ambin Massif. Here, the rock mass is mainly constituted of hard rock such as micaschists and gneiss and is classified with a fair to good quality (Barla and Antolini 2014; Parisi et al. 2017). The relevant tunnel depth and the competent rock mass portend the likely occurrence of brittle failure and justify the application of the methodological flow shown in Fig. 1. Indeed, based on preliminary geological-geotechnical investigations of the Ambin Massif through the 7 km-long exploratory tunnel of "La Maddalena", the possibility of occurrence of brittle failure and rockbursts was assessed (Parisi et al. 2017). The exploratory tunnel was completed in February 2017 using a 6.3 diameter TBM under exceptionally high overburden of more than 2000 m. Stress release phenomena were observed when overburdens exceeded around 400 m. The stand-up times of the unsupported rock started to decrease and rock fragments/wedges collapsed before support could be installed. Parisi et al. (2017) report that a significant rockburst event was observed at an overburden of 950 m. The rock mass experienced a sudden brittle failure at the tunnel crown and invert with a damage depth of 1-1.5 m, while minor damage

took place at the sidewalls. Brittle failure was systematically observed in the crown and invert as excavation progressed, although not as strong as described before.

It is well known that the initial stress state is very difficult to be assessed and is characterized by high uncertainty. Therefore, in the following, both a stress ratio of 1 (isotropic, σ_v=σ_h=66.4 MPa) and 1.5 (anisotropic, σ_v=66.4 MPa and σ_h=99.6 MPa) will be analysed.

According to the first block in Fig. 1, the TBI is calculated to predict the brittle failure proneness of the tunnel-rock mass system. The values of the necessary input parameters (listed in Table 1) are indicated in Table 2 and were estimated based on the information found in the literature. Using these parameters, the values Λ_{duc}=1.61 and Λ_{brt}=0.76 are determined for k_0=1 (case of isotropic original stress state), while for k_0=1.5 (anisotropic original stress state) the values Λ_{duc}=1.29 and Λ_{brt}=0.43 are obtained. In both scenarios, Λ_{duc} takes on a physically meaningless value (inadmissible) as it exceeds 1, whereas Λ_{brt} falls within the admissible range. Consequently, the final result is TBI=1, representing the maximum prevalence of the brittle failure mechanism over the ductile one.

Following the positive outcome of the TBI calculation with reference to brittle failure occurrence, the analysis can proceed with the quantitative phase which is carried out by adopting FDEM, specifically by means of the software Irazu (Geomechanica Inc. 2023). The analyses carried out by Martinelli and Insana (2024) for the same case study will be here described. They simulated a 2D, homogeneous, plane strain cross-section of the circular tunnel at a depth of 2500 m in the Ambin Massif. The construction of the numerical model, as described in Section 4, accounted for the fact that fracture trajectories are restricted along the edges of finite elements and that larger elements will require more energy to fracture. Thus, the mesh setup was appropriately designed, with constant strain triangular elements' sizes ranging from 0.1 to 5 m. The micaschists and gneiss rock mass mechanical parameters adopted, as well as the penalty values, are summarized in Table 2. Elastic properties were assigned to finite elements over the whole domain, while strength properties and penalties were assigned to cohesive crack elements. A unit viscous damping was assumed. The in-situ state of stress was assigned based on the two cases of stress ratio declared above. Since the tunnel is deep, gravitational gradients can be neglected. Gravity is off, so only the effect due to spalling is reflected in the calculated displacements.

Table 2 Mechanical and numerical parameters adopted for the computation of TBI and in the simulations.

Parameter	**Value**	**Property**	**Value**
Rock mass Young's modulus, E (GPa)	35	Mode I fracture energy, G_{fI} (N/m)	32.5
Rock mass Poisson's ratio, ν (-)	0.25	Mode II fracture energy, G_{fII} (N/m)	650
Geological Strength Index, GSI (-)	90	Fracture penalty, p_f (GPa)	17.5
Rock mass tensile strength, σ_{ti} (MPa)	10	Normal penalty, p_n (GPa·m)	35
Intact rock UCS, σ_{ci} (MPa)	144	Tangential penalty, p_t (GPa/m)	8.5
Rock mass friction coefficient, f_r (-)	0.7	Density, γ (kg/m^3)	2500
Rock mass cohesion, c (MPa)	23	Intact rock shear modulus, G_i (GPa)	24
In situ stress ratio, k (-)	1, 1.5	Equivalent thickness of the rock, λ (m)	0.21
Rock mass Drucker-Prager parameter, A (MPa)	5.14	Maximum geostatic stress, σ_∞ (MPa)	66.4, 99.6
Rock mass Drucker-Prager parameter, B (-)	0.51		

After running a FE analysis and applying the initial state of stress, the FDEM run follows. Tunnel excavation was simulated using the core replacement procedure previously discussed. The Young's modulus was softened linearly over 75,000 steps. Then, the inner core triangular finite elements were instantaneously removed and the state of the surrounding crack elements was set to "broken". Fig. 2 and Fig. 3 show the fracture evolution and the final pattern retrieved after the excavation of the deep unsupported 10.4 m diameter tunnel in a brittle rock mass. Spalling occurring around the tunnel is quite extended already with k_0=1 (around 2.5-5 m). This evidence points out the necessity of considering a support to be installed to prevent the fall of blocks from the contour of the cavity. Considering the condition with k_0=1.5, the extension of the spalling phenomenon increases, as expected. A damaged zone along the direction of the minor principal stress is shown, with the development of fractures at the tunnel crown and invert. In these zones the progressive extension and coalescence of fractures evolved up to the generation of a notched geometry and eventually to unstable rock slabs, leading both to the complete collapse of the tunnel's roof and to extensive damage at the invert.

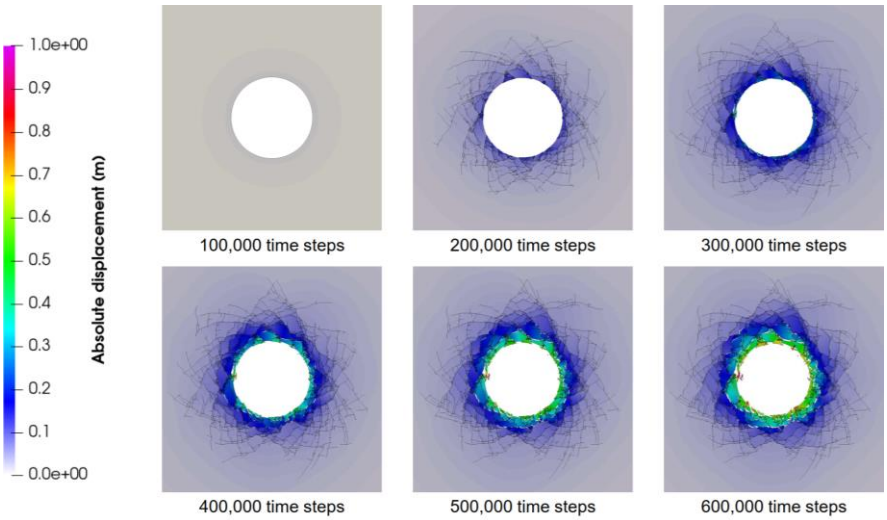

Fig. 2 Simulated evolution of displacement contour and fracture pattern for k_0=1.0 (Martinelli and Insana 2024).

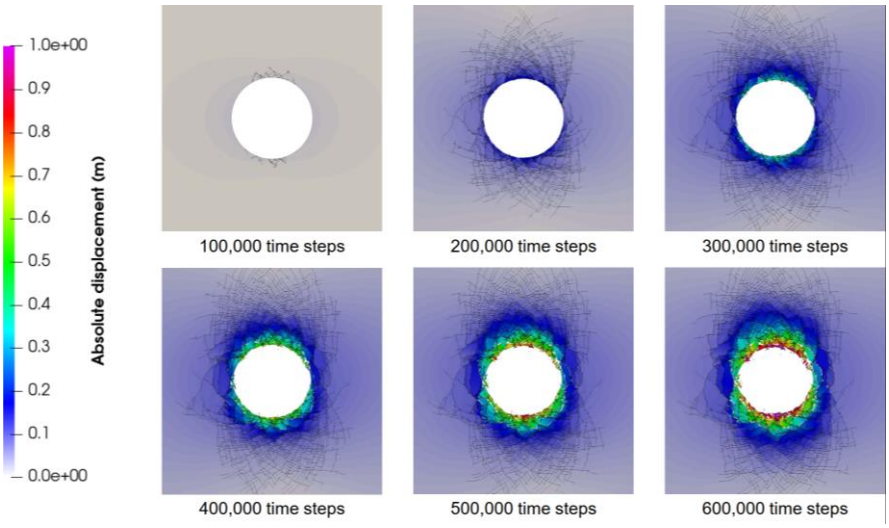

Fig. 3 Simulated evolution of displacement contour and fracture pattern for k_0=1.5 (Martinelli and Insana 2024).

6 Conclusions

The proposed design methodology for assessing brittle failure in deep tunnels provides a rational, comprehensive approach to predict and quantify the occurrence of brittle failure in deep tunnels. This rational method integrates the Tunnel Brittleness Index (TBI) for qualitative assessment and the Finite Discrete Element Method (FDEM) for quantitative analysis. The TBI serves as a valuable tool in the early stages of tunnel design, enabling engineers to anticipate brittle failure. The subsequent FDEM analysis provides detailed insights into the fracture patterns and spalling phenomena. Such insights may allow to make informed decisions regarding excavation techniques and support systems with the aim to optimize tunnel stability and safety.

The application of this methodology to the Turin-Lyon Base tunnel case study demonstrates its practical utility, though only comparisons with evidences from the La Maddalena exploratory tunnel are possible at the time of the writing of this paper. Future research and case studies will further refine and validate this methodology, ensuring its applicability and effectiveness in identifying potential failure mechanisms and guiding the implementation of appropriate support measures.

References

Askaripour M, Saeidi A, Rouleau A, Mercier-Langevin P (2022) Rockburst in underground excavations: A review of mechanism, classification, and prediction methods. Underground Space 7(4):577–607

Barla M, Piovano G, Grasselli G (2012) Rock Slide Simulation with the Combined Finite Discrete Element Method, International Journal of Geomechanics 12: 13. 10.1061/(ASCE)GM.1943-5622.0000204

Barla M, Antolini F (2014) Combined Finite-Discrete numerical modeling of rock spalling in tunnels. 14th International conference of IACMAG, Kyoto, Japan, 21-24 September 2014

Cai M (2013) Principles of rock support in burst-prone ground. Tunn. Undergr. Sp. Tech. 36:46–56

Cai M, Brown E (2017) Challenges in the mining and utilization of deep mineral resources. Eng. 3:432–433.

Chen Y, Zhang J, Zhang J, Xu B, Zhang L, Li W (2021) Rockburst precursors and the dynamic failure mechanism of the deep tunnel: A review. Energies 14(22): 7548

Cook NGW (1976) Seismicity associated with mining. Engineering Geology 10(2-4):99–122

Diederichs M (2007) Mechanistic interpretation and practical application of damage and spalling prediction criteria for deep tunneling. Can. Geotech. J. 44: 1082-1116. https://doi.org/10.1139/T07-033

Geomechanica Inc (2023) Irazu 2D Geomechanical Simulation Software. V. 6.1. Theory Manual.

Gong F, Wang Y, Luo S (2020) Rockburst proneness criteria for rock materials: Review and new insights. Journal of Central South University 27:2793–2821.

He M, Ribeiro e Sousa L, Miranda T, Zhu G (2015) Rockburst laboratory tests database - application of data mining techniques. Engineering Geology 185:116–130

He M, Cheng T, Qiao Y, Li H (2022) A review of rockburst: Experiments, theories, and simulations. Journal of Rock Mechanics and Geotechnical Engineering 15(5):1312–1353

Hoek E, Kaiser PK, Bawden WF (2000) Support of Underground Excavations in Hard Rock. CRC Press, London

Kaiser PK, McCreath DR, Tannant DD (1996). Canadian rockburst support handbook. Geomechanics Research Center, Sudbury

Li S, Feng X-T, Li Z, Chen B, Zhang C, Zhou H (2012) In situ monitoring of rockburst nucleation and evolution in the deeply buried tunnels of Jinping II hydropower station. Engineering Geology 137-138: 85–96

Li T, Ma C, Zhu M, Meng L, Chen G (2017) Geomechanical types and mechanical analyses of rockbursts. Engineering Geology 222:72–83.

Liang Z, Liu X, Zhang Y, Tang C (2013) Analysis of precursors prior to rock burst in granite tunnel using acoustic emission and far infrared monitoring. Mathematical Problems in Engineering:1–10

Lisjak A, Liu Q, Zhao O, Mahabadi OK, Grasselli G (2013) Numerical simulation of acustic emissions in brittle rocks by two dimensional finite-discrete analysis. Geophysical Journal International 195(1): 423-443.

Lisjak A, Grasselli G, Vietor T (2014) Continuum-discontinuum analysis of failure mechanism around unsupported circular excavations in anisotropic clay shales. Int. J. Rock Mech. Min. Sci. 65: 96-115.

Liu X, Zhan S, Zhang Y, Wang X, Liang Z, Tian B (2018) The Mechanical and Fracturing of Rockburst in Tunnel and Its Acoustic Emission Characteristics. Shock and Vibration 3503940:1-11.

Mahabadi OK, Lisjak A, Munjiza A, Grasselli G (2012) Y-Geo: New Combined Finite-Discrete Element Numerical Code for Geomechanical Applications. Int. J. of Geomech. 12(6): 676–688.

Martin CD, Read RS, Martino JB (1997) Observation of brittle failure around a circular test tunnel. Int J Rock Mech Min Sci 34(7): 1065–73

Martin CD, Kaiser PK, Christiansson R (2003) Stress, instability and design of underground excavations. International Journal of Rock Mechanics & Mining Sciences 40: 1027–1047

Martinelli D, Insana A (2024) Application of a Finite-Discrete Element Method Code for Modelling Rock Spalling in Tunnels: The Case of the Lyon-Turin Base Tunnel. Appl. Sci. 14(591):1-15

Milan L (2024a) A new approach for predicting brittle or ductile failure of rock in deep excavations. PhD Thesis at Politecnico di Torino, Torino, Italy

Milan L (2024b) GitHub repository https://github.com/LorenzoMilan/TBI-Computation_ App

Milan L, Barbero M, Borri-Brunetto M (2025) A new method to assess the possibility of brittle failure of rock induced by deep excavations. Int. J. Numer. Anal. Meth. Geomech.

Munjiza A, Owen DRJ, Bicanic N (1995) A combined finite-discrete element method in transient dynamics of fracturing solids. Engineering Computations 12(2): 145-174.

Naji AM, Emad MZ, Rehman H, Yoo H (2019) Geological and geomechanical heterogeneity in deep hydropower tunnels: A rock burst failure case study. Tunn. Undergr. Sp. Tech. 84: 507-521.

Ortlepp WD, Stacey TR (1994) Rockburst mechanisms in tunnels and shafts. Tunn. Undergr. Sp. Tech. 9(1): 59-65

Ortlepp WD (1997) Rock fracture and rockbursts – An illustrative study. Monograph Series M9, South African Institute of Min. Metall, Johannesburg.

Ortlepp WD (2001) The behaviour of tunnels at great depth under large static and dynamic pressures. Tunn. Undergr. Sp. Tech. 16: 41-48

Parisi ME, Brino L, Gilli P, Fornari E, Martinotti G, Lo Russo S (2017) La Maddalena exploratory tunnel. Geomechanics and Tunnelling 10(3): 265-274

Piovano G, Barla M, Barla M (2011) FEM/DEM modeling of a slope instability on a circular sliding surface. Computer methods for Geomechanics: frontiers and new applications, 13th International conference of IACMAG, Melbourne, Australia, 9-11 May 2011, Vol. 2.